

# Electron Conditioning of Technical Aluminium Surfaces: Effect on the Secondary Electron Yield

F. Le Pimpec, F. King, R.E. Kirby  
SLAC, 2575 Sand Hill Road, Menlo Park, CA 94025

10th December 2004

## Abstract

The effect of electron conditioning on commercially aluminium alloys 1100 and 6063 were investigated. Contrary to the assumption that electron conditioning, if performed long enough, can reduce and stabilize the SEY to low values ( $\leq 1.3$ , value of many pure elements [1]), the SEY of aluminium did not go lower than 1.8. In fact, it reincreases with continued electron exposure dose.

## 1 Introduction

In the framework of the ILC electron cloud suppression, studies on secondary electron emission (SEE) from technical surfaces are ongoing.

In this brief paper we will present secondary electron yield (SEY),  $\delta$ , results obtained from two technical surfaces : aluminium alloys 1100 and 6063. We compare these results to other data obtained elsewhere.

It is known, from the literature, that a metallic aluminium surface has a  $\delta_{max}$  below 1 [1]. However, its technical surface is oxidized, and the  $\delta_{max}$  can be well above 2.5. This value might not be compatible with the running of a charged positively particle beam, and it becomes necessary to find a way to lower the yield of such surfaces. Coatings and electron or ion conditioning are two ways of achieving this goal [2] [3].

## 2 Experiment Description and Methodology

The system, sketch in Fig.1, and experimental methodology used to measure the secondary electron yield have been described thoroughly in [2]. Hence, we will summarize the description of the SEY system.

---

<sup>0</sup>Work supported by the Department of Energy Contract DE-AC02-76SF00515

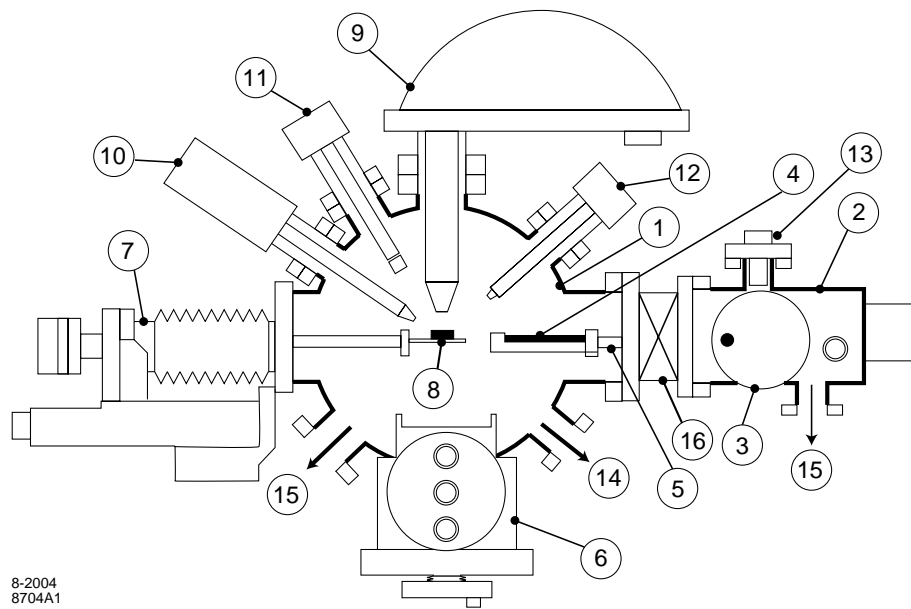


Figure 1: Experimental setup

- |  |                                  |
|--|----------------------------------|
| 1. Analysis chamber                              | 9. Electrostatic energy analyzer |
| 2. Loadlock chamber                              | 10. X-ray source                 |
| 3. Sample plate entry                            | 11. SEY/SEM electron gun         |
| 4. Sample transfer plate                         | 12. Microfocus ion gun           |
| 5. Rack and pinion travel                        | 13. Sputter ion gun              |
| 6. Sample plate stage                            | 14. To pressure gauges and RGA   |
| 7. XYZ $\theta$ Omniax <sup>TM</sup> manipulator | 15. To vacuum pumps              |
| 8. Sample on XYZ $\theta$                        | 16. Gate valve                   |

The system is composed of two coupled stainless steel ultra high vacuum (UHV) chambers where the pressure is in the low  $10^{-10}$  Torr scale in the measurement chamber and high  $10^{-9}$  Torr scale in the "load lock" chamber. Samples, individually screwed to a carrier plate, are loaded first onto an aluminium transfer plate in the load lock chamber, evacuated to the low  $10^{-8}$  Torr scale, and then transferred into the measurement chamber.

The sample to be measured is installed on a special manipulator arm. The feature of this arm allow us to bake the loaded sample, and the temperature is recorded by the use of type C thermocouples. The back of the samples are heated by electron bombardment. This is achieved by biasing a tungsten filament negatively.

The electronic circuit for SEY measurement is that presented in Fig.2 [4]. The energy of the computer-controlled electron beam coming from the gun is decoupled from the target measurement circuitry. However, the ground is common to both. The target is attached to a bias voltage supply and an electrometer connected in series to the data gathering computer Analog Digital Converter (ADC). Measurements were made with a Keithley 6487, a high resolution picoammeter with internal variable  $\pm 505$  V supply and IEEE-488 interface. The 6487 has several filter modes which were turned off for our

measurements. The integration time for each current reading is  $167 \mu\text{s}$ , which is the minimum value for the instrument. The current was sampled one hundred times; the mean and standard deviation were returned from the picoameter to the computer.

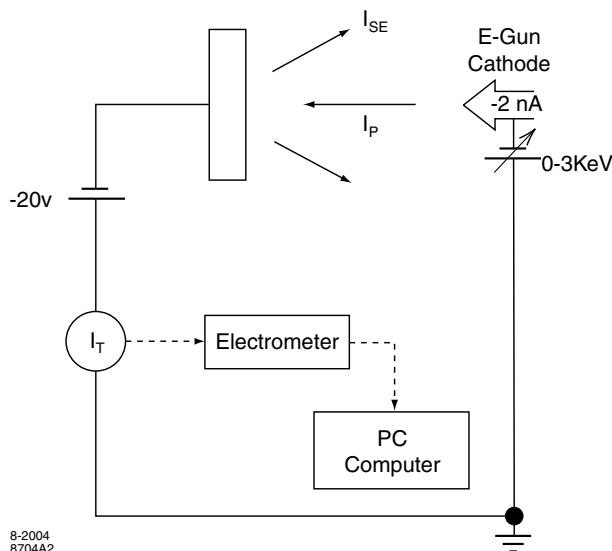


Figure 2: Electronic circuitry used to measure the secondary emission yield

The SEY ( $\delta$ ) definition is determined from equation 1. In practice equation 2 is used because it contains parameters measured directly in the experiment.

$$\delta = \frac{\text{Number of electrons leaving the surface}}{\text{Number of incident electrons}} \quad (1) \quad \delta = 1 - \frac{I_T}{I_P} \quad (2)$$

Where  $I_P$  is the primary current (the current leaving the electron gun and impinging on the surface of the sample) and  $I_T$  is the total current measured on the sample ( $I_T = I_P + I_S$ ).  $I_S$  is the secondary electron current leaving the target. The reproducibility of the experiment is around 2%.

### 3 Effect of 130 eV Electron Bombardment on the SEY of Al

#### 3.1 History of Aluminium 1100 and 6063 samples

Aluminium 1100 is composed, at the minimum, of 99% Al. Copper is present in the range of 0.2% to 0.5%. The other elements, present as impurities, are manganese, zinc, silicon and iron. Aluminium 6063 is composed of 98.9% Al, 0.45% to 0.9% of Mg, and 0.2% to 0.6% of Si. Other impurities for Al 1100 are also present in 6063, including copper.

The samples were chemically cleaned for UHV use, but not deliberately passivated, and then kept in a dry nitrogen purged box.

In an attempt to create an aluminium-nitride (AlN) thin film, for the purpose of lowering the SEY, the Al 1100 sample was heated to  $200^\circ\text{C}$  with pure hot  $200^\circ\text{C}$  nitrogen gas blown on it. The results were not encouraging (too low temperature), so the sample

surface was scraped clean in air with a tungsten carbide tool, and was loaded in the SEY system. XPS confirmed that the sample was quite clean, but air oxidized.

Two Al 6063 samples were also tested. The first sample will be referred to as Al 6063. This sample was also scraped clean before loading into the SEY system. The second sample, which is not scraped, will be referred as the LER Al 6063 sample. This sample comes from a piece of the extruded Low Energy Ring (LER) chamber made of Al 6063. This piece was UHV cleaned and stored in air for years and then loaded as it in the SEY system. The LER accelerator provides the positron beam in the SLAC B-factory.

### 3.2 Secondary Electron Yield of Al 1100

The SEY results obtained by exposing the Al 1100 sample to an electron conditioning beam of 130 eV kinetic energy are presented in Fig.3 and 4. In the NLC positron damping ring the average energy of the electrons from the cloud was computed to be 130 eV [3]. The SEY values were measured for a primary beam impinging the Al surface at 23° from normal incidence. During the conditioning, the pressure rose to  $2.10^{-9}$  Torr equivalent  $N_2$ , due to electron stimulated desorption (ESD) from the sample. As the dosing continued the pressure diminished to  $5.10^{-10}$  Torr. The effect of electron conditioning of ESD on Al was, and still is, widely documented [5].

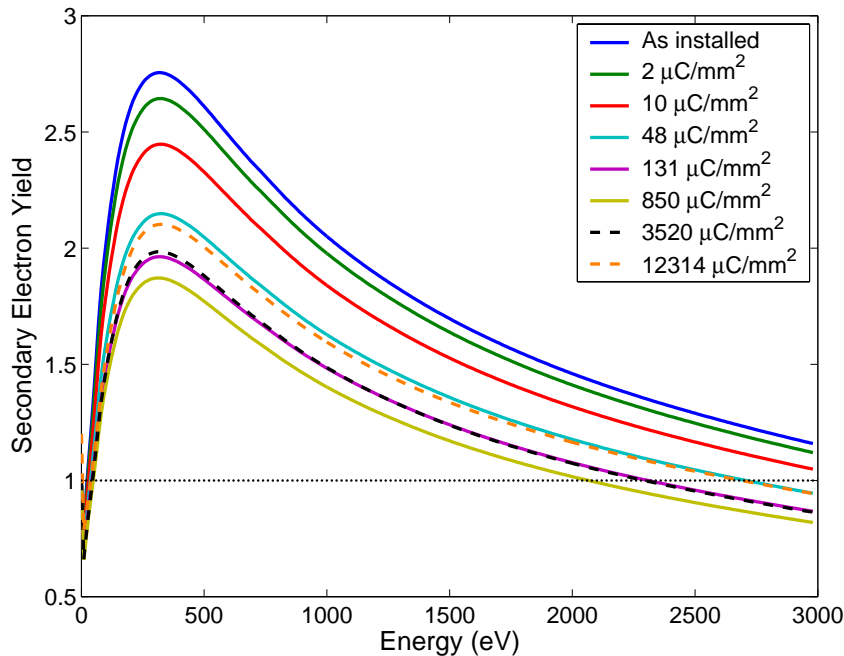


Figure 3: Al 1100 exposed to electron conditioning. The primary electron beam was impinging at 23° from normal incidence

During the first  $1000 \mu\text{C}/\text{mm}^2$ , the SEY of the Al 1100 sample goes down as expected. However, we can see that this trend seems to level off, suggesting that the conditioning of aluminium is a very long process, Fig.4. However, the next point at  $3520 \mu\text{C}/\text{mm}^2$  shows an increase of the SEY, hence an increase of the  $\delta_{max}$ .

This increase is contrary to expectation, i.e, normally yield decreases with dose. In order to check the consistency of the value, the sample was moved 5 mm, and a second

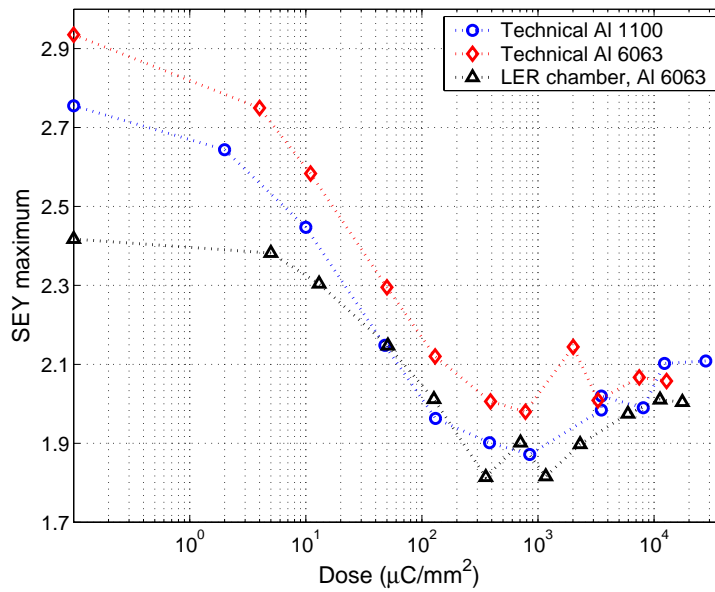


Figure 4: SEY max vs the electron dose received by the Al alloy samples, measured at 23° from normal incidence

point was collected, Fig.5. The results agreed and we continued the conditioning to still higher dose.

To check the measurement system reproducibility, a previously conditioned and measured NEG sample was installed on the holder and re-measured. A NEG sample can be used as an SEY reference sample, especially when baked. The SEY curve and the  $\delta_{max}$  obtained from the NEG were those expected, hence ruling out any instrumental problem.

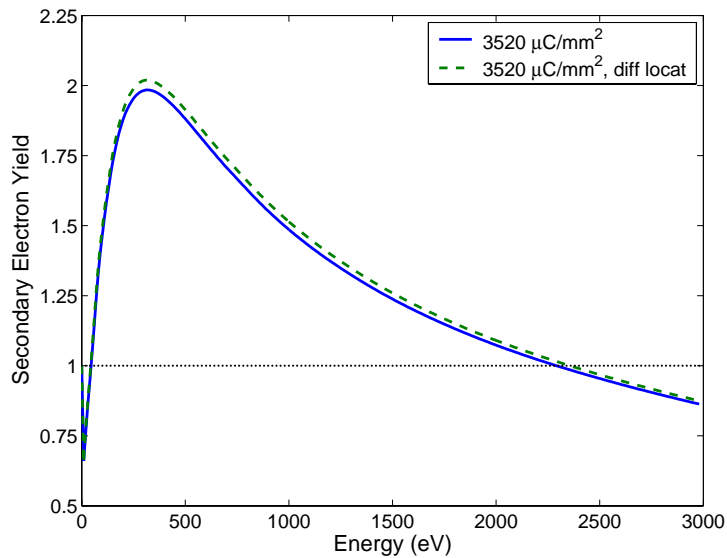


Figure 5: SEY of Al 1100 at two different locations, same electron dose of 3520  $\mu\text{C}/\text{mm}^2$

The last value for the  $\delta_{max}$ , reached after 40  $\text{mC}/\text{mm}^2$  of electron exposure was 2.1. Thus, the conclusion that we had reached saturation, at the previous point, was hasty.

### 3.3 Secondary Electron Yield of Al 6063

The SEY results obtained by exposing the Al 6063 sample to an electron conditioning beam of 130 eV kinetic energy are presented in Fig.4, 6 and Fig.7.

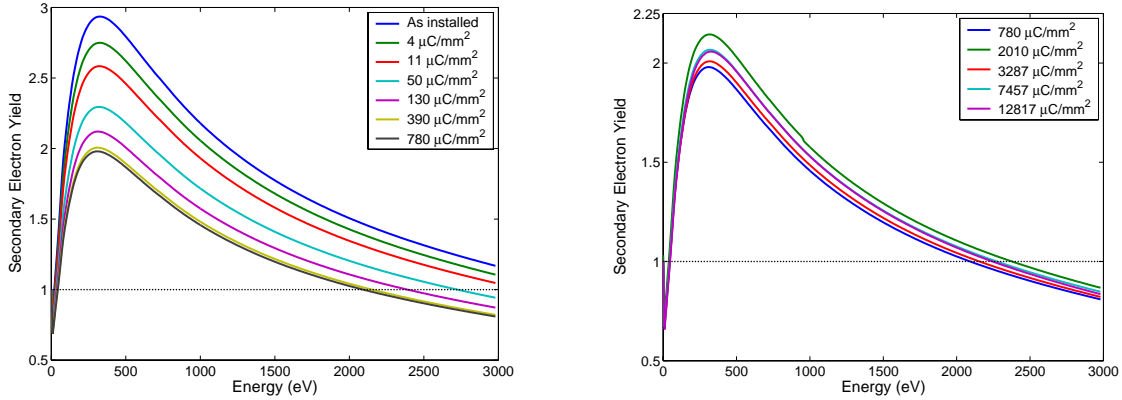


Figure 6: Al 6063 exposed to electron conditioning. SEY values are monotonically decreasing on the left plot and monotonically increasing on the right plot

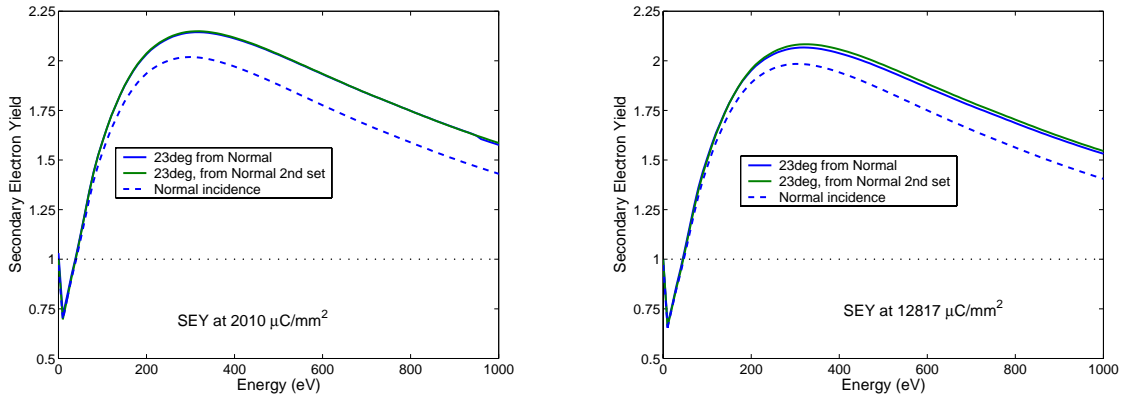


Figure 7: SEY of Al 6063 at 23° and normal incidence

As observed for the Al 1100 sample, the SEY of the Al 6063 also decreases with the increasing dose until reaching a dose of  $\sim 800 \mu\text{C}/\text{mm}^2$ , Fig.4 and Fig.6, left plot. After this point the SEY increases, but not smoothly, Fig.4. The SEY max at a dose of  $2010 \mu\text{C}/\text{mm}^2$  reached a value of 2.13. Subsequent measurements at this dose are in very good agreement with the first set of data Fig.7, left plot. The next points at  $3000 \mu\text{C}/\text{mm}^2$ ,  $7000 \mu\text{C}/\text{mm}^2$  and  $12000 \mu\text{C}/\text{mm}^2$  have been also measured twice, Fig.7 right plot as an example, and were found to agree within 1.5%. The SEY at those subsequent doses are less than the one obtained at  $2000 \mu\text{C}/\text{mm}^2$ , Fig.4 and 6, right plot. This jump is currently not understood.

### 3.4 Secondary Electron Yield of the LER Al 6063

The SEY results obtained by exposing the LER Al 6063 sample to an electron conditioning beam of 130 eV kinetic energy are presented in Fig.8, 9 and Fig.10.

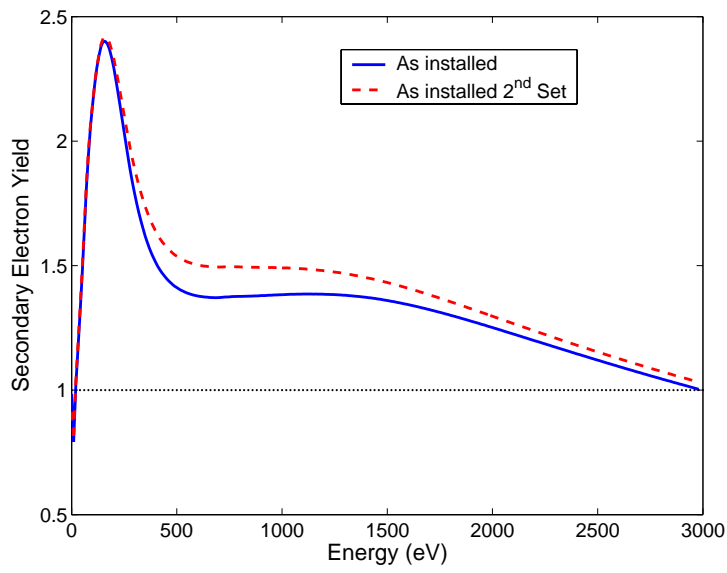


Figure 8: SEY of LER Al 6063 as installed. Curve shapes are due to charging of the oxide layer

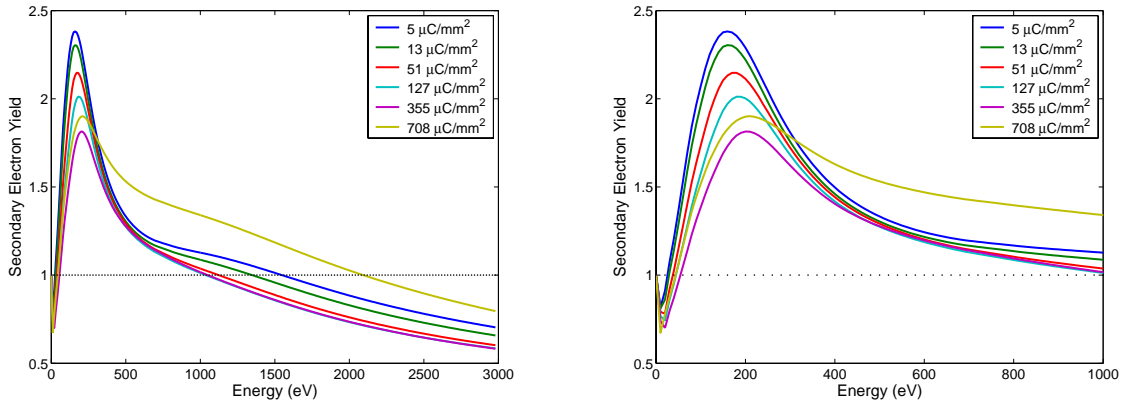


Figure 9: LER Al 6063 exposed to electron conditioning, first part of the conditioning. Values are monotonically decreasing. Detail of the SEY between 0-1 keV right plots

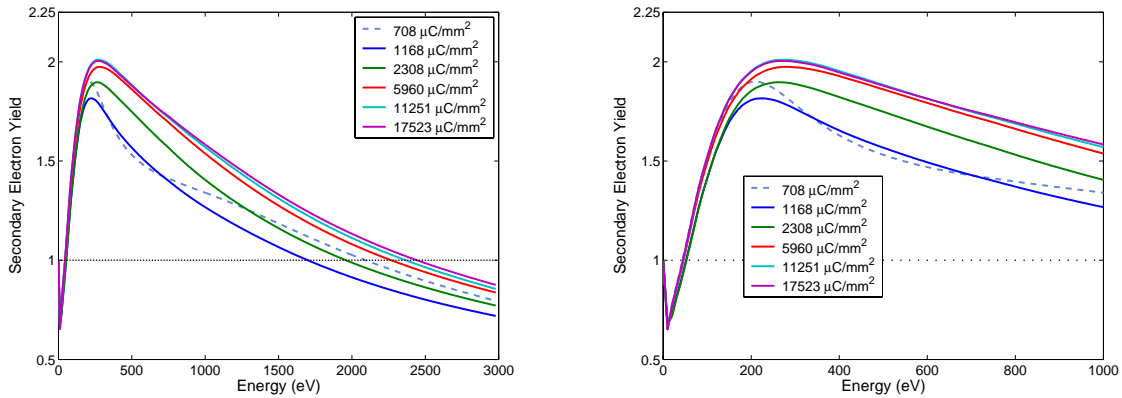


Figure 10: LER Al 6063 exposed to electron conditioning, Second part of the conditioning. Values are monotonically increasing. Detailed of the SEY between 0-1 keV right plots

As observed for the Al 1100 and the Al 6063 scraped samples, the SEY of the LER sample decreases with the increasing dose until reaching a dose of  $\sim 800 \mu\text{C}/\text{mm}^2$ , Fig.4 and Fig.9, left plot. After this point the SEY increases, but not smoothly, Fig.4 and Fig.10. On the second part of the dosing, Fig.10, the evolution of the SEY changes drastically from the as-installed shapes and values Fig.8. The  $\delta_{max}$  shifts from being reached at 160 eV to being reached at 270 eV. The curves after reaching a dose of  $708 \mu\text{C}/\text{mm}^2$  becomes similar as the SEY plots from clean scraped Al 1100 and 6063.

### 3.5 Are the results believable ?

Despite the fact that our results seems contradictory to common belief, previous data collected at CERN (Conseil Européen pour la Recherche Nucléaire) [6] supports, indirectly, our findings. The conditioning curves, Fig.11, of the  $300^\circ\text{C}$  pre-baked aluminium sample (blue circle) show a dip, which bottoms around 1.8, data taken at normal incidence. The SEY of the last aluminium point, around  $7 \text{ mC}/\text{mm}^2$ , is in very good agreement with our value obtained at  $8 \text{ mC}/\text{mm}^2$ , Fig.4.

In some other data, collected at ANL (Argonne National Laboratory) on an Al 6063 sample, the  $\delta_{max}$  achieved after an electron dose exposure of  $350 \text{ nA}/\text{cm}^2$  for 5h (equivalent to  $63 \mu\text{C}/\text{mm}^2$ ) at an energy of 100 eV is around 2.1 [7]. From these comparisons and the system check, by the use of a NEG, we are confident in the results obtained above  $8 \text{ mC}/\text{mm}^2$ .

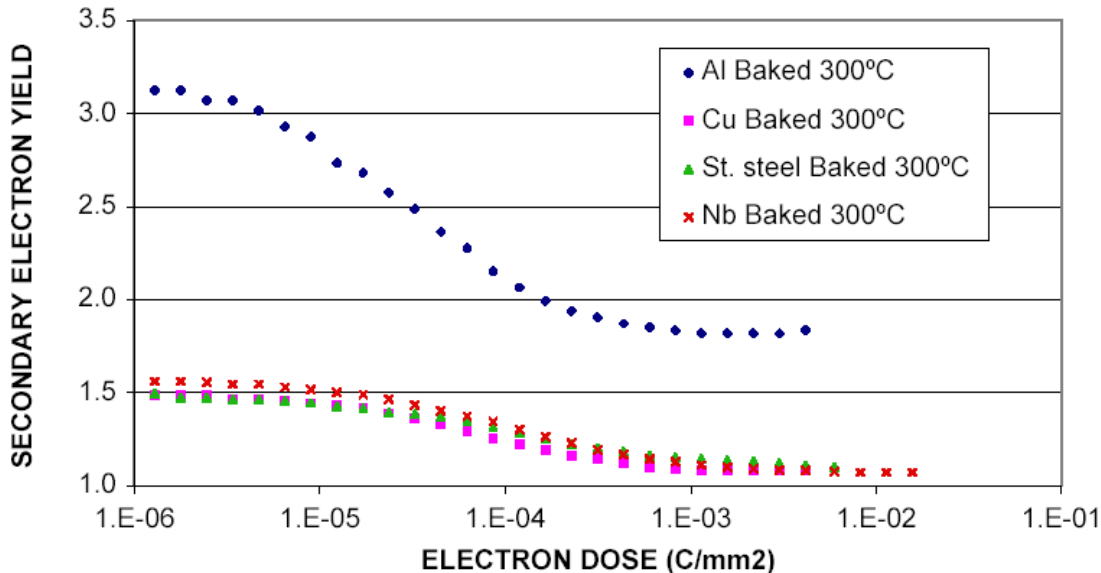


Figure 11: SEY of baked technical surfaces conditioned by electrons from ref.[6]

## 4 XPS study of the C1s and Al2p peak

### 4.1 XPS study of Al 1100

XPS analysis was carried out to observe the evolution of the carbon and aluminium chemistry during the electron conditioning, Fig.12. The spectra are shifted vertically



from one another for clarity. The "Al as installed" spectra is located at the top of Fig.12, and the "27880  $\mu\text{C}/\text{mm}^2$ " at its bottom.

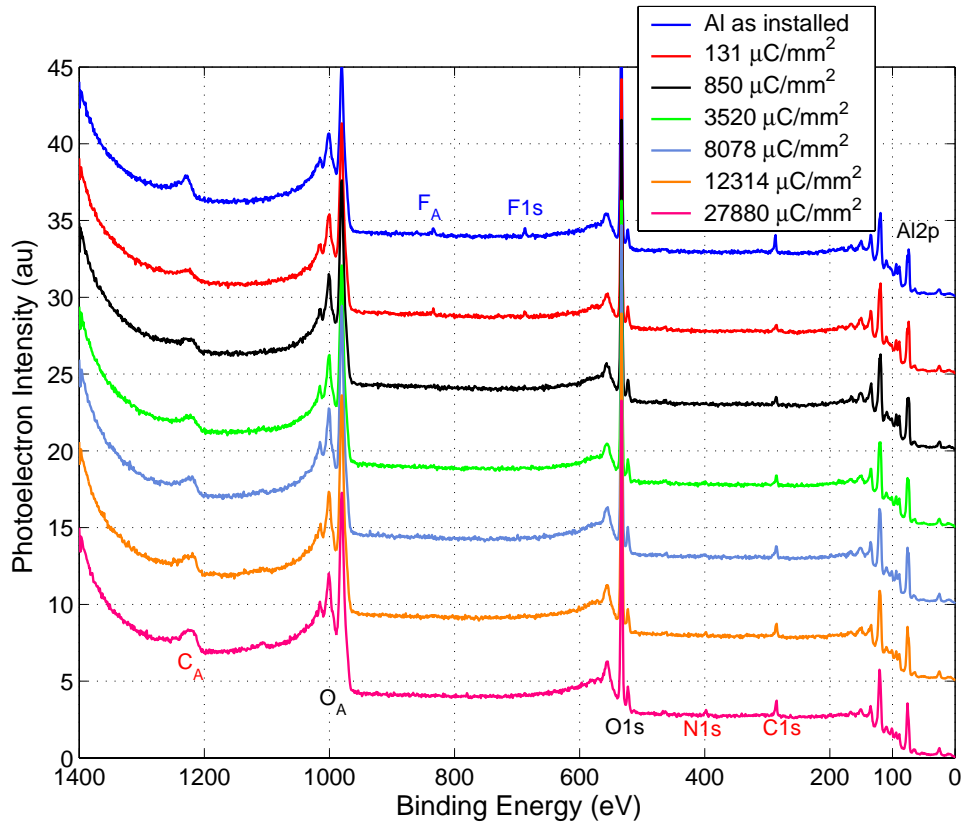


Figure 12: XPS survey of the Al 1100 sample during electron conditioning. "A" subscript indicates Auger peak. Top curve: as installed sample; near BE axis: sample after 27880  $\mu\text{C}/\text{mm}^2$  electron dosing

From the "as installed" condition to the end of the conditioning, a few obvious observations can be made. First of all, the "as installed" sample is contaminated by fluorine (F). The sample was not passivated and was thoroughly scraped. We must assume that this F is present in the air and reacts very quickly with a pure Al surface, hence getting imbedded in the oxide layer. Fluorine compounds are used heavily in the semiconductor industry to prepare silicon wafers. Our location is in the heart of this industry.

During the initial conditioning the F1s (685 eV) quickly disappears, Fig.13. However, a peak of nitrogen then appears, N1s (398 eV), Fig.14.

It is possible that during our attempt to create an AlN film, a proportion of N was absorbed in the bulk of the Al 1100. During conditioning, the surface is "cleaned-up", by ESD and the mobility of the N is enhanced, thence diffusing to the surface or near subsurface(1-5 nm depth). This N concentration, being very small, 2 at%, is unlikely to have influenced the behaviour of the aluminium with respect to the SEY.

A survey of the Al2p was carried out during the conditioning. The high-energy resolution spectra are shown in Fig.15. A pure Al surface will present a single peak at 73 eV, and a pure Al<sub>2</sub>O<sub>3</sub> surface will have one peak at 74.5 eV [8].

The "as installed" Al2p is peaked at 73.5 eV and 76.5 eV, shown at a resolution of 0.5 eV for a step scan energy of 1 eV. Those peaks match the Al2p location of a pure

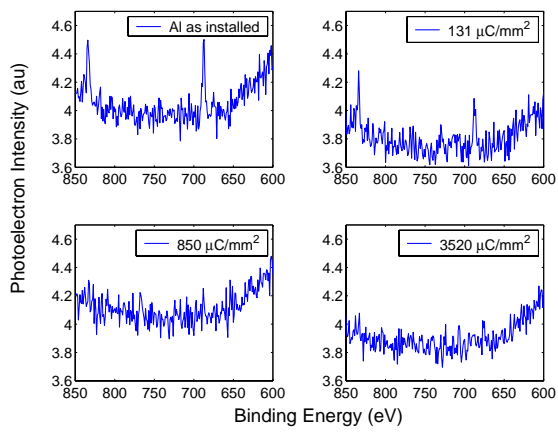


Figure 13: Disappearance of F1s (685 eV) and  $F_A$  (Auger) during initial electron conditioning

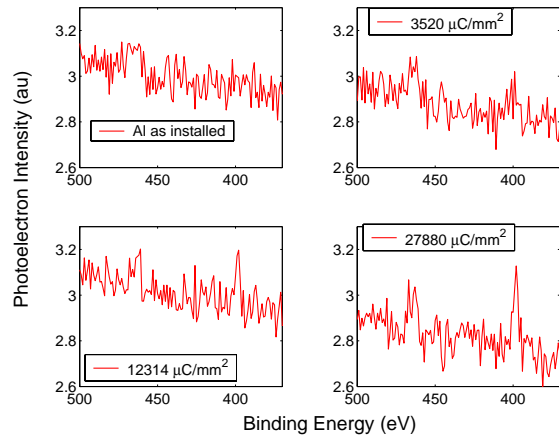


Figure 14: Emergence of N1s (400 eV) during late electron conditioning

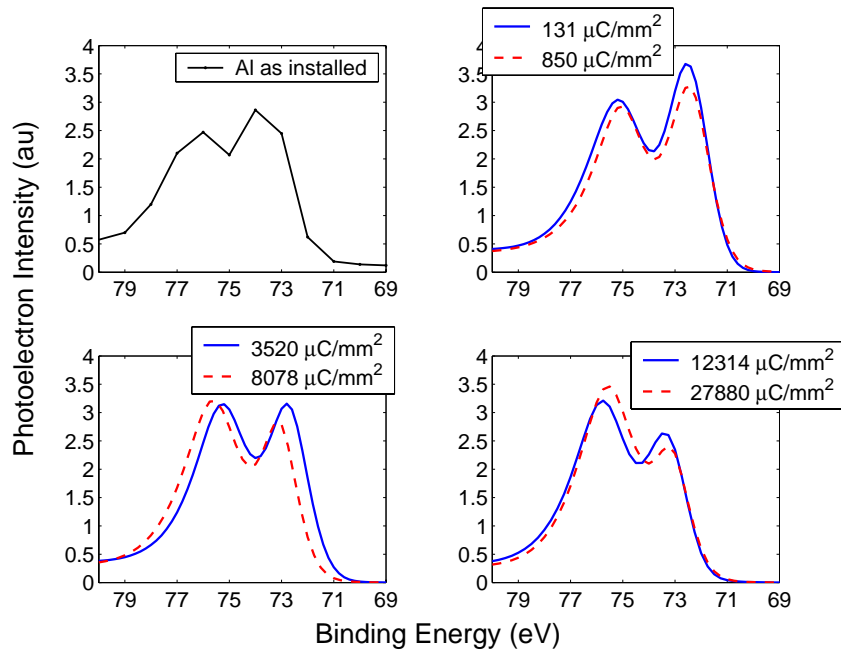


Figure 15: Detailed spectra of the Al2p during the electron conditioning

Al surface and a halogenated Al surface. As the fluorine disappears from the surface, the spectrum shifts to lower binding energy and presents the characteristic of a thin aluminium oxide film (less than 5 nm) on an aluminium substrate. Very similar curves on an Al 6063 alloy sample can be found in [7], where the peaks are representatives of the pure Al (73 eV BE) and the oxidized Al (76 eV BE). Moreover, during conditioning of our Al 1100 sample, the relative intensities of the peaks changes during the conditioning. The aluminium peak (73 eV) becomes smaller than the oxide peak (75 eV).

From this last observation we hypothesize that we are thickening the aluminium oxide layer by decomposing carbon monoxide and dioxide from the residual gas and, by rearranging the bonds on the surface, the oxygen displaces the carbon covering the aluminium.

This interpretation for the Al is supported by the C1s spectra, Fig.16. The C of the "as installed" Al is peaked at 287.5 eV, but also has a peak at 291 eV. This high binding energy (BE) is reminiscent of carbon passivated by HF acid which shows a peak at 289 eV [8].  $CF_2$  compounds also will have a peak at 292 eV [8]. After an accumulated dose of  $850 \mu C/mm^2$ , the F disappeared, and we saw a shift from 291 eV to 288 eV, location of oxidized C1s. During conditioning, the peak not only gets shifted further toward 285 eV (marker of an amorphous/graphitic C surface) but also the peak intensity rose. This shows that the C is transformed from an oxidized state to its amorphous/graphitic form.

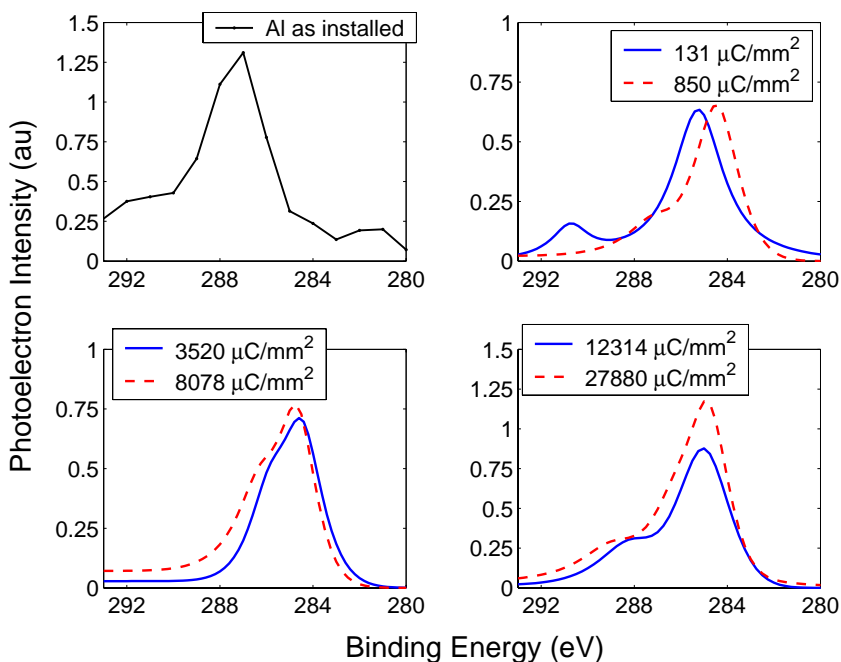


Figure 16: Detailed spectrum of the C1s during electron conditioning

## 4.2 XPS of Al 6063

XPS analysis of Al 6063 was carried out to observe the evolution of the carbon and aluminium chemistry during the electron conditioning, Fig.17. The spectra are shifted vertically from one another for clarity. The "Al as installed" spectra is located at the top of Fig.17, and the " $12817 \mu C/mm^2$ " near the BE axis.

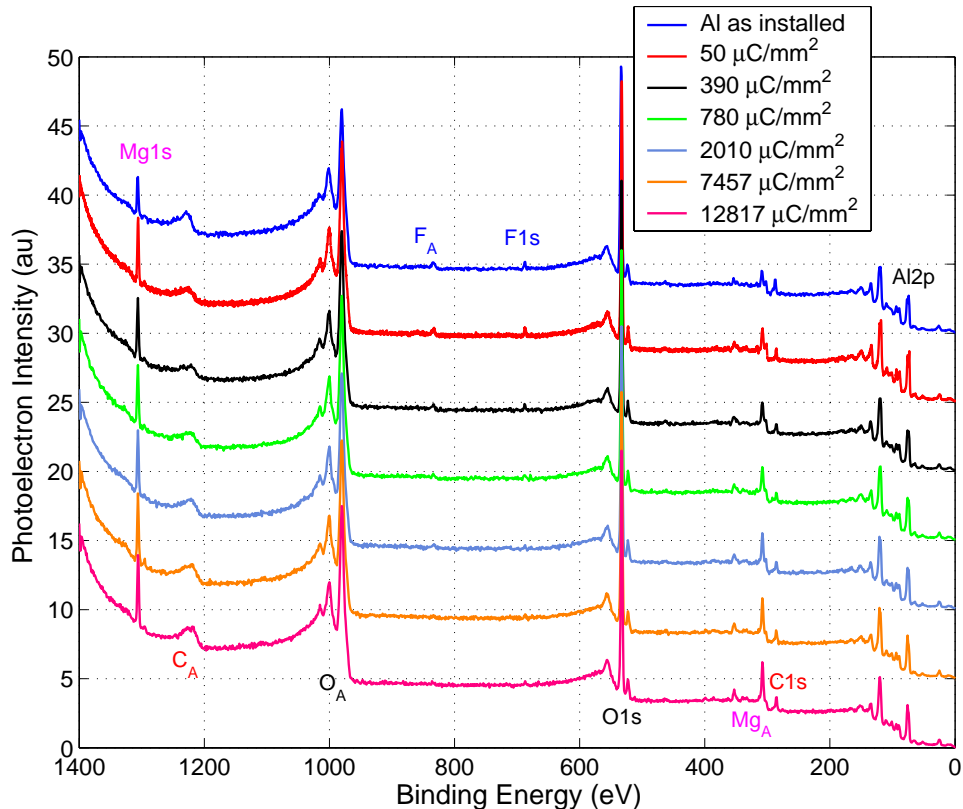


Figure 17: XPS survey of Al 6063 sample during electron conditioning. Top curve: as installed sample; near BE axis: sample after  $12817 \mu\text{C}/\text{mm}^2$  electron dosing

The observations on Al 6063 are similar of those on Al 1100. The "as installed" Al2p is peaked at 73.5 eV and 76 eV, for a step scan energy of 0.25 eV, Fig.18. Those peaks match the location of a pure Al surface and a halogenated Al surface. As the fluorine disappears from the surface, due to electron bombardment, the spectrum shifts to lower binding energy and presents the characteristic of a thin aluminium oxide film (less than 5 nm) on an aluminium substrate, Fig.19. The shift in energy, is also accompanied with a change in intensities between the peaks, as it was observed on the Al 1100, Fig.15. In [7], the XPS spectra from the technical Al 6063 sample, exposed to the effect of a running accelerator beam, shows a shift toward lower BE of the oxidized peak. The intensity of the oxidized Al peak before running the beam is higher than the pure Al peak. It does not seem that the relative intensities between the pure metal and oxidized metal varies at the end of the beam exposure. The XPS spectra before and after exposure to the beam of the facing away side of the sample shows no variation.

The presence of significant amounts of Mg inside the 6063 alloy complicates the interpretation of the XPS data. Its continuous presence on the surface is marked by its 1s peak at 1306 eV BE, Fig.17. Mg is also a very good oxygen getter and its evolution was monitored by observing the 301 eV and 308 eV BE KLL Auger peaks, Fig.20. A pure Mg surface will present an higher Auger peak at 301 eV than at 308 eV, [8]; this picture is reversed for an oxidized Mg [9]. During the conditioning we see that the 308 eV peaks increases and the 301 eV disappears.

An XPS spectrum from a piece of LER vacuum chamber, made of Al 6063, was also taken. The spectrum does not show any pure metal peak at 301 eV. This piece of LER

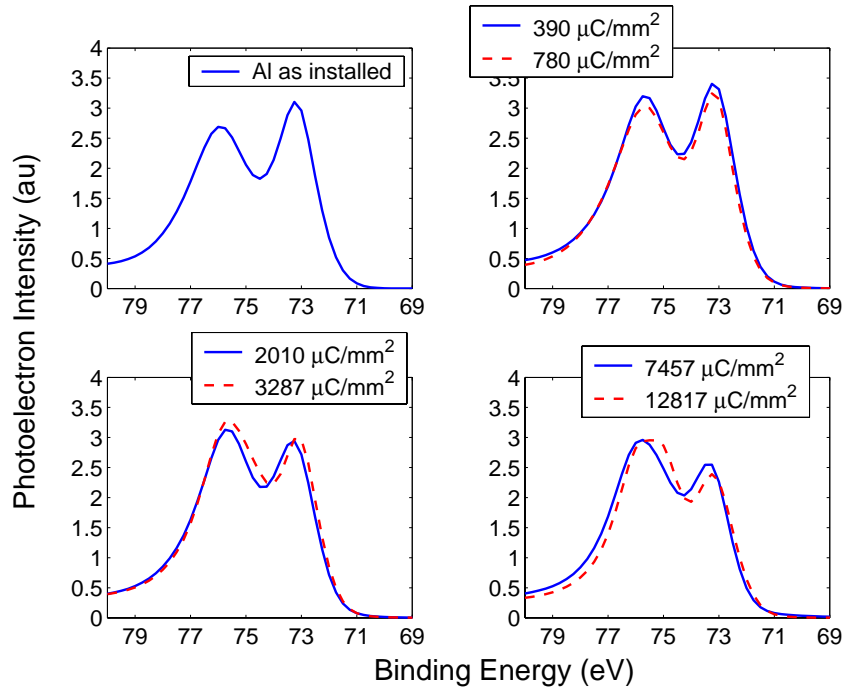


Figure 18: Detailed spectra of the Al 2p during electron conditioning of Al 6063

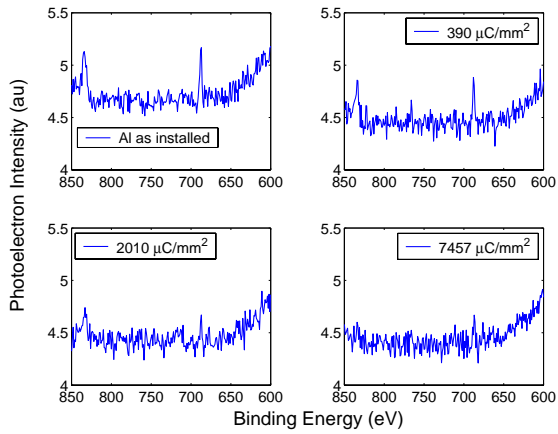


Figure 19: Disappearance of F1s (685 eV) during electron conditioning

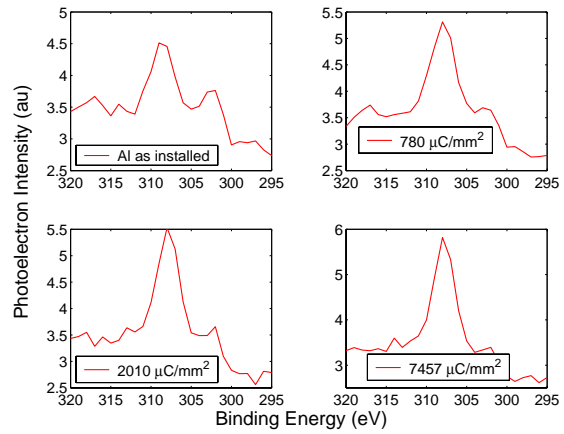


Figure 20: Modification of Auger  $KL_{23}L_{23}$  Mg peaks (301 eV and 308 eV) during electron conditioning

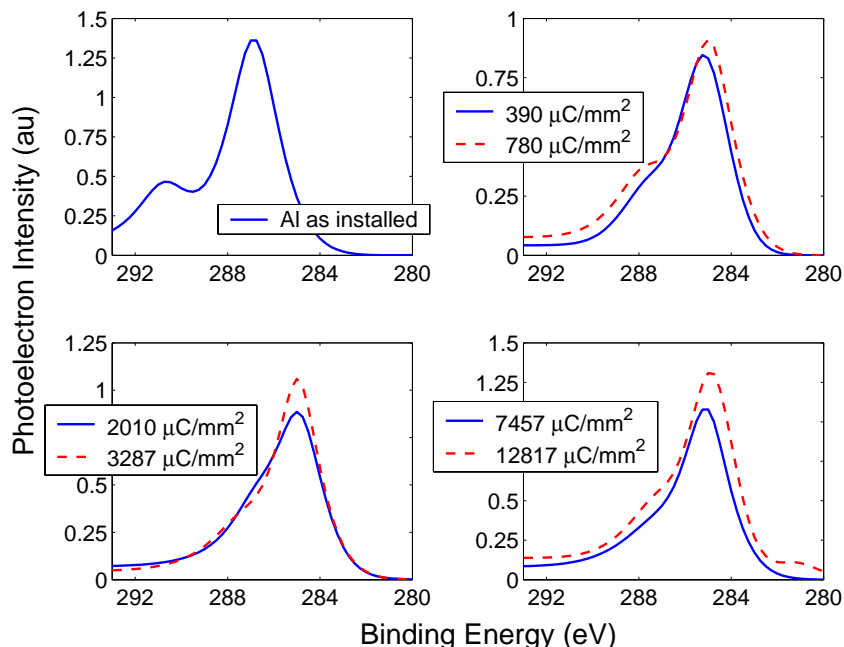


Figure 21: Detailed spectrum of the C1s during electron conditioning of Al 6063

chamber was kept in air for many years, hence built a thick natural Al and Mg oxide, probably  $\text{Mg}(\text{OH})_2$  [9]. All of these observations support our preceding hypothesis, in which we stated that, during electron conditioning an oxide layer grows on the technical surface.

The Al 6063 XPS spectrum for the C1s (285 eV BE), Fig.21, is similar to the one obtained for the Al 1100, Fig.16. The results obtained on the two alloy surfaces show the same chemistry evolution.

### 4.3 XPS of LER Al 6063

XPS analysis of LER Al 6063 was carried out to observe the evolution of the carbon and aluminium chemistry during the electron conditioning, Fig.22. The spectra are shifted vertically from one another for clarity. The "Al as installed" spectra is located at the top of Fig.22, and the "12817  $\mu\text{C}/\text{mm}^2$ " near the BE axis. The survey shows that a non scraped Al 6063 has a different chemistry at the surface than the scraped Al 6063 Fig.17. There is, for example, no presence of fluorine (685 eV) on the surface.

The Al2p spectra of the non scraped Al 6063 sample coming from the LER chamber shows the presence of one peak at 78 eV. A non oxidized Al surface has an Al2p peak, peaked at 73 eV [10]. As no fluorine is present, this peak could be the mark of an oxide. However, as seen in [8]  $\text{Al}_2\text{O}_3$  is peaked at 74.5 eV, however from [10],  $\text{Al}_2\text{O}_3$  is peaked at 75.6 eV and  $\text{Al}(\text{OH})_3$  at 76.5 eV. None of the oxide explain the shift to the higher (78 eV) BE. However, as the electron dose received by the sample increased, the peak shifts to lower BE and broadens. This broadening is the signature of the rearrangement of the aluminium oxide.

The LER Al 6063 XPS spectrum for the C1s (285 eV BE), Fig.24, is similar to the one obtained for the Al 1100 and scraped Al 6063, Fig.16 and Fig.21. Their evolution

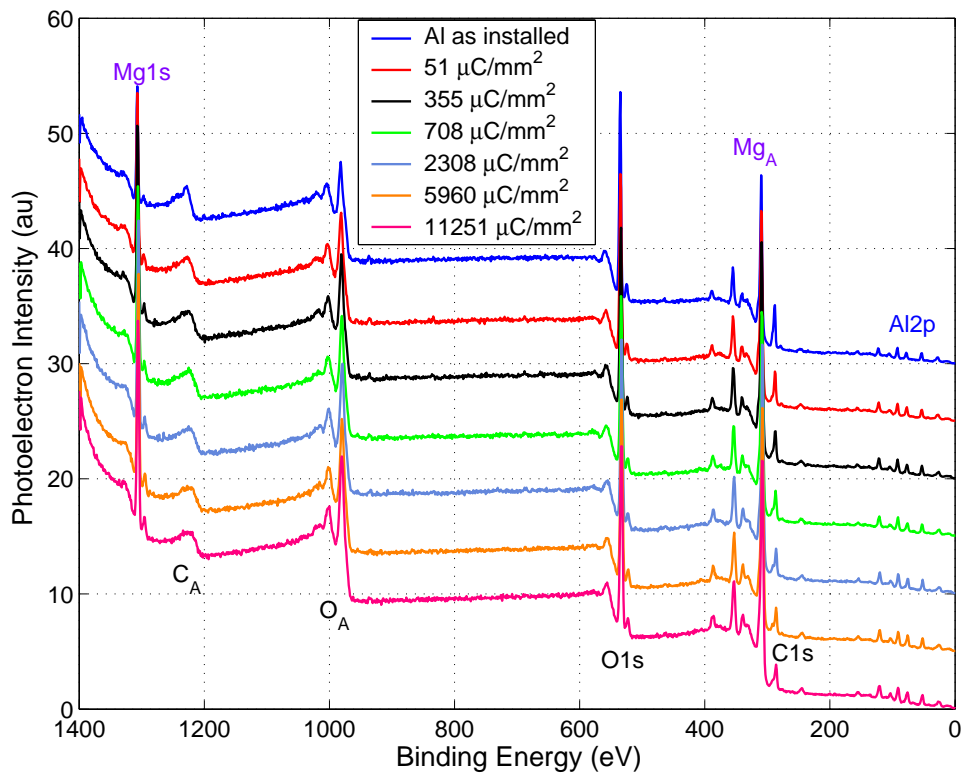


Figure 22: XPS survey of LER (Al 6063) sample during electron conditioning. Top curve: as installed sample; near BE axis: sample after 11251  $\mu\text{C}/\text{mm}^2$  electron dosing

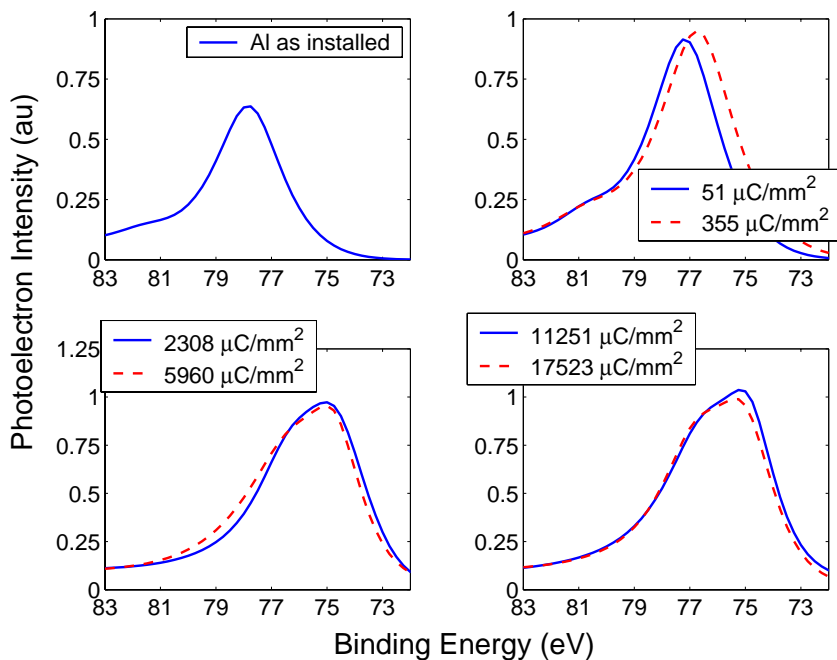


Figure 23: Detailed spectra of the Al 2p during electron conditioning of the LER Al 6063 sample

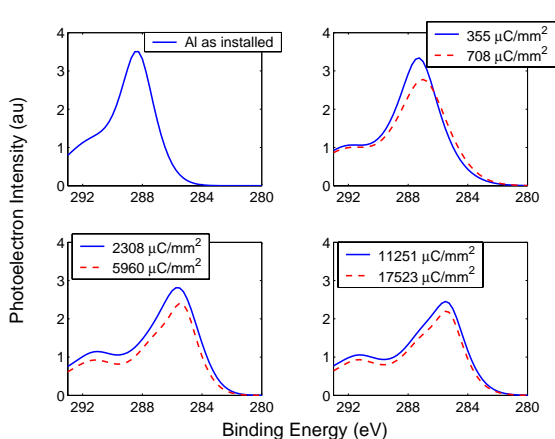


Figure 24: Evolution of C1s during electron conditioning of the LER Al 6063

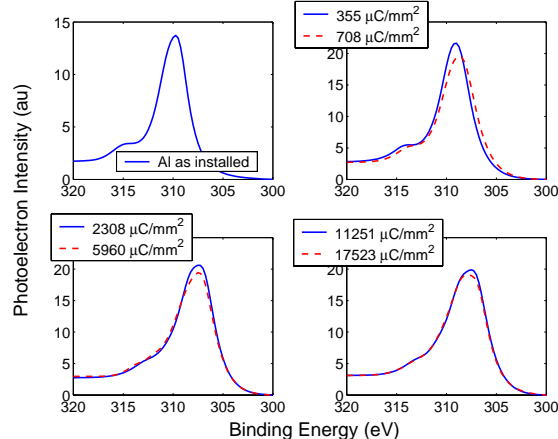


Figure 25: Modification of Auger  $KL_{23}L_{23}$  Mg peaks (301 eV and 308 eV) during electron conditioning

during electron bombardment are also similar, the oxidized carbon being transformed into a more graphitic form. It was hypothesized that the C peak at 291 eV for the scraped Al technical surfaces was due to the presence of F at the surface. As no F is present on the LER Al 6063, the deformed shape of the C must be due to different oxygen bonding. Oxide containing hydroxide-type (C-O-H) produces a chemical shift of 1.5 eV from the graphitic carbon (285 eV BE). Carbonyl (C=O) and carboxyl (COOH) have chemical shift of 3.0 eV and 4.5 eV, respectively [11]. As this sample was kept in air for years, all oxidation state of the surface are likely. The intensity of the "as installed" C1s peak of the LER 6063 sample, Fig.22, is higher than that for the scraped 6063 and 1100 samples, Fig.17 and Fig.12, respectively. A fair amount of carbonate ( $CO_3$ ) can also be present, with the BE of this compound on a native Al oxide peaked at 291 eV [10]. However, it is stated in [12] that aluminium carbonate is not expected to be formed in presence of  $CO_2$  and water.

The Mg  $KL_{23}L_{23}$  exhibits a shift in energy toward a lower BE in function of the dose received, Fig.25. The intensity measured by the electron analyser of the XPS varies from an as installed piece to the conditioning at a dose of  $708 \mu C/mm^2$ . From this point on the variation in intensities are minimal. The Mg2p of this LER sample was also displaced toward higher BE (54 eV) and shifts toward lower BE (52 eV) during electron conditioning. Even, if  $MgCO_3$  was present on the surface (BE : 52 eV [10]) the 54 eV BE cannot be explained by chemistry alone. In fact, when comparing the binding energies of several peaks from the LER sample spectrum from the as installed state versus the  $11251 \mu C/mm^2$  electron dosing state, Fig.22, we found that the peaks of the  $11251 \mu C/mm^2$  spectrum have shifted 2 eV to lower BE. This implies that the LER sample as installed must have charge up during XPS measurement.

## 5 Explaining the dip in the SEY curve

The "as installed" aluminium surface is contaminated by components in the air, hence a "carbonaceous oxide" layer forms. During electron conditioning, the ESD process cleans



up and modifies the chemistry of the surface. Unpolymerized hydrocarbons and water are known to promote a high SEY [13].

During conditioning the SEY curve goes down, Fig.4, as modification and removal of the surface contamination takes place. The SEY curves is the sum of aluminium-oxide (high SEY) an aluminium surface (low SEY) and graphitic carbon. At some point, the aluminium surface contribution prevails, as the oxide layer is not yet formed or arranged properly. That is the dip of the curves. Past this point, the contribution of the forming aluminium oxide starts prevailing, hence raising the SEY.

This model is also supported by others SEY measurements, with a 3 keV electron beam energy, of an evaporated Al and grown  $\text{Al}_2\text{O}_3$  thin film [14] [15]. The SEY, at 3 keV, of an Al thin film exposed to oxygen shows a dip, and this is independent of the oxygen pressure in the vacuum chamber [15].

For comparison, no dip is seen on copper because copper oxide ( $\text{Cu}_2\text{O}$ ) has a lower SEY than the pure Cu [1] [16].

Finally, it is not known how much higher doses of electron on the surface will affect the SEY. It is possible, following our hypothesis from our XPS observation, that we are building an aluminium oxide layer, therefore the SEY will keep increasing. The  $\delta_{max}$  could reach any values between 2 and 9, values of  $\text{Al}_2\text{O}_3$  (layer) [1].

The usual mechanism for oxidation of metals involves diffusion of atomic oxygen through the growing oxide layer toward the underlying metal, which is then oxidized. Thus, the rate-limiting step for oxide growth, via the Mott-Carbrera mechanism, is diffusion of oxygen through oxide.

## 6 Conclusion

We have reported on the effects of conditioning, with electrons of 130 eV, on three technical surfaces, aluminium 1100, aluminium 6063 and aluminium 6063 heavily oxidized. We have observed that a technical aluminium surface does not seem to condition to saturation with dose, as it is commonly observed for many other technical surfaces and thin films. The low dose part, below a  $\text{mC}/\text{mm}^2$ , of our results appear normal, Fig.4. High doses cause oxide growth and the yield rises, contrary to expected experience. XPS characterization of the chemistry happening on the surface during conditioning supports our model.

In the framework of the electron cloud problem, the choice of the technical surface to be used as vacuum chambers is clear. Non-coated, or otherwise untreated, use of aluminium is a bad idea, as its conditioned SEY might not go consistently below 2. However, in an accelerator, ions of few hundred eV can be made present. Their effect on the surface, from a conditioning standpoint, is not yet known.

## 7 Acknowledgments

We would like to thanks G. Collet, for his help with the aluminium nitridation experiment. We also would like to thanks N. Hilleret for useful comments.

# References

- [1] David R. Lide, editor. *Handbook of Chemistry and Physics*. 74<sup>th</sup> edition. CRC PRESS, 1994.
- [2] F. Le Pimpec, F. King, R.E. Kirby, M. Pivi. Secondary Electron Yield Measurements of TiN Coating and TiZrV Getter Film. Technical report, SLAC TN03-052, 2003.
- [3] F. Le Pimpec, F. King, R.E. Kirby, M. Pivi, G.Rumolo. The Continuing Story of Secondary Electron Yield Measurements from TiN Coating and TiZrV Getter Film. Technical report, SLAC TN04-046, 2004.
- [4] R.E. Kirby F.K. King. Secondary Emission Yield from PEP-II accelerator material. *Nuclear Instruments and Methods in Physics Research A*, A469, 2001.
- [5] M.Q. Ding and E.M. Williams. Electron Stimulated Desorption of gases at technological surfaces of aluminium. *Vacuum*, 39:463, 1989.
- [6] N. Hilleret et al. The Secondary Electron Yield of Technical Materials and its Variation with Surface Treatments. In *EPAC , Vienna, Austria*, 2000.
- [7] R. Rosenberg et al. X-ray photoelectron spectroscopy and secondary electron yield analysis of Al and Cu samples exposed to an accelerator environment. *Journal of Vacuum Science and Technology*, A21(5), 2003.
- [8] *Handbook of X-Ray Photoelectron Spectroscopy*. Perkin-Elmer Corporation, 1992.
- [9] K. Asami and S. Ono. Quantitative X-Ray Photoelectron Spectroscopy Characterization of Magnesium Oxidized in Air. *Journal of the Electrochemical Society*, 147(4):1408, 2000.
- [10] *Handbooks of Monochromatic XPS Spectra*. Volume 1 - The Elements and Native Oxides. XPS International, Inc., 1999.
- [11] Y. Xie and P.M.A Sherwood. Coatings of Aluminum Oxide and Magnesium Oxide on Carbon Fiber Surfaces. *Chem. Matter.*, 6:650, 1994.
- [12] A.N. Buckley. Threshold Al KLL Auger Spectra of Oxidized Aluminium foils. *Surface and Interface Analysis*, 35:922, 2003.
- [13] J. Halbritter. On Changes of Secondary Emission by Resonant Tunneling via Adsorbates. *Journal de Physique*, 45:C2-315, 1984.
- [14] M. Steinbatz et al. Electron emission yield from thin Al and insulating layers induced by 3 MeV He<sup>2+</sup> and 3 keV electron impact. *Nuclear Instruments and Methods in Physics Research B*, 193:638, 2002.
- [15] O. Benka, M. Steinbatz. Oxidation of aluminum studied by secondary electron emission. *Surface Science*, 525:207, 2003.
- [16] I. Bojko, N. Hilleret, C. Scheuerlein. Influence of air exposures and thermal treatments on the secondary electron yield of copper. *Journal of Vacuum Science and Technology*, A18(3), 2000.